ASCE Author Proofs

Important Notice to Authors

Attached is a PDF proof of your forthcoming article in **Journal of Bridge Engineering**. The manuscript ID number is **BEENG-2703**.

No further publication processing will occur until we receive your response to this proof. Please return any corrections within 48 hours of receiving the download email. Your paper will be published in its final form upon receipt of these corrections. You will have no further opportunities to review your proof or to request changes after this stage.

Information and Instructions

- The graphics in your proof have been down-sampled to produce a more manageable file size and generally represent the online presentation. Higher resolution versions will appear in print.
- Proofread your article carefully, as responsibility for detecting errors lies with the author.
- Mark or cite all corrections on your proof copy only.
- Corrections should be sent within 48 hours after receipt of this message.
- If no errors are detected, **you are still required to inform us that the paper is okay** to be published as is.
- You will receive a message confirming receipt of your corrections within 48 hours.

Color Figures

Figures containing color will usually appear in color in the online journal. All figures will be grayscale in the printed journal unless you have agreed to pay the color figure surcharge and the relevant figure caption indicates “(Color)”. For figures that will be in color online but grayscale in print, please ensure that the text and captions do not describe the figures using the colors of the online version.

If you have indicated that you will be printing color figures in color (or choosing Open Access), you will receive an email from ASCE Author Services with a link to the publication fee payment system. Until payment is received, your article will not be published.

Reprints

If you would like to order reprints of your article, please visit http://www.asce.org/reprints.

Questions and Comments to Address

The red numbers in the margins correspond to queries listed on the last page of your proof. Please address each of these queries when responding with your proof corrections.

Return your Proof Corrections

- Web: If you accessed this proof online, follow the instructions on the Web page to submit corrections.
- E-mail: Send corrections to ASCE.Production@cenveo.com. Include the manuscript ID **BEENG-2703** in the subject line.

ASCE Open Access

Authors may choose to publish their papers through ASCE Open Access, making the paper freely available to all readers via the ASCE Library website. ASCE Open Access papers will be published under the Creative Commons-Attribution Only (CC-BY) License. The fee for this service is $1,750, and must be paid prior to publication. If you indicate Yes, you will receive a follow-up message with payment instructions. If you indicate No, your paper will be published in the typical subscribed-access section of the Journal.

Selecting Yes does not commit you to publishing your article as Open Access. You will have the option to cancel the Open Access process later. If you are unsure, we recommend selecting Yes. If you select No now, your paper will be published online shortly after your proof corrections are received, and you will no longer have the ability to publish your article as Open Access.

If you have indicated that you will be choosing Open Access, (or printing color figures in color), you will receive an email from ASCE Author Services with a link to the publication fee payment system. Until payment is received, your article will not be published.

Adding Comments and Notes to Your PDF

To facilitate electronic transmittal of corrections, we encourage authors to use the comments and notes features in Adobe Acrobat or the free Adobe Reader software (see note below regarding acceptable versions). The PDF provided has been "comment-enabled," which allows you to use the text editing and annotation features.

When you open your PDF in **<u>Adobe Acrobat</u>**, the comments/notes/edit tools are shown on the top tool bars (icons may differ slightly among versions from what is shown below). The important features to know are the following:

Use the **Text Edits** tool (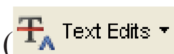

) to insert, replace, or delete text.

- To **insert text**, place your cursor at a point in the text and select "Insert Text at Cursor" from the text edits menu. Type your additional text in the pop-up box.

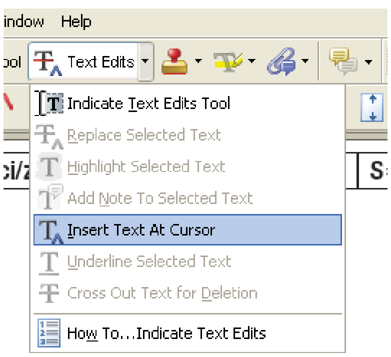

- To **replace text**, highlight the text to be changed, select "Replace Selected text" from the text edit menu, and type the new text in the pop-up box.

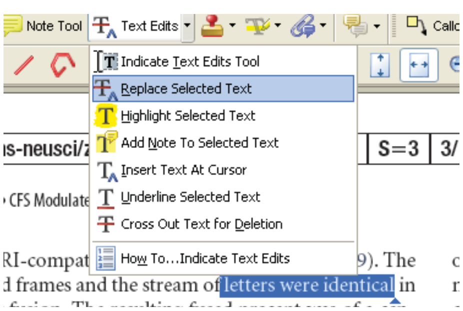

- To **delete text**, highlight the text to be deleted and select "Cross Out Text for Deletion" from the text edits menus (see graphic above).

Use the Sticky Note tool (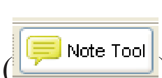

) to describe changes that need to be made (e.g., changes in bold, italics, or capitalization use; altering or replacing a figure; general comments) or to answer a question or approve a change that was posed by the editor. Beware that comment bubbles can shift. They are not recommended as a primary text editing tool.

Use the **Callout tool** () to point directly to changes that need to be made. Try to put the callout box in an area of white space so that you do not obscure the text, as in the example below:

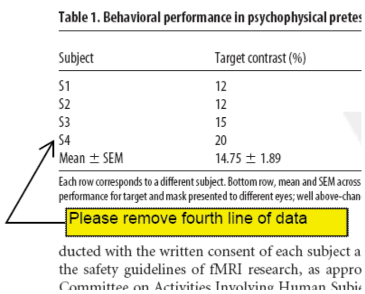

Á Use the **Highlight tool** (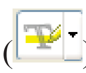) to indicate font problems, bad breaks, and other textual inconsistencies. You can describe the problem with the Callout tool (above), a sticky note, or by double clicking highlighted text (a pop-up window will appear where you can add your comment).

To access the annotation tools in the free **<u>Adobe Reader</u>** software, select the "view" menu and then "Comment" as shown below. You can also access the text edit tools in Adobe Reader through the "View" menu.

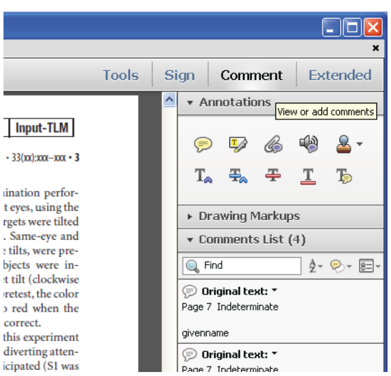

<u>Note:</u> To use the comments/notes features on this PDF you will need Adobe Reader version 10 or higher. This program is freely available and can be downloaded from http://get.adobe.com/reader/.

Novel Demountable Shear Connector for Accelerated Disassembly, Repair, or Replacement of Precast Steel-Concrete Composite Bridges

Ahmed S. H. Suwaed[1] and Theodore L. Karavasilis[2]

Abstract: A novel demountable shear connector for precast steel-concrete composite bridges is presented. The connector uses high-strength steel bolts, which are fastened to the top flange of the steel beam with the aid of a special locking nut configuration that prevents bolts from slipping within their holes. Moreover, the connector promotes accelerated construction and overcomes the typical construction tolerance issues of precast structures. Most importantly, the connector allows bridge disassembly. Therefore, it can address different bridge deterioration scenarios with minimum disturbance to traffic flow including the following: (1) precast deck panels can be rapidly uplifted and replaced; (2) connectors can be rapidly removed and replaced; and (3) steel beams can be replaced, whereas precast decks and shear connectors can be reused. A series of push-out tests are conducted to assess the behavior of the connector and quantify the effect of important parameters. The experimental results show shear resistance, stiffness, and slip capacity significantly higher than those of welded shear studs along with superior stiffness and strength against slab uplift. Identical tests reveal negligible scatter in the shear load-slip displacement behavior. A design equation is proposed to predict the shear resistance with absolute error less than 8%. **DOI: 10.1061/(ASCE)BE.1943-5592.0001080.**

Introduction

During the last two decades, rapid deterioration of bridges has become a major issue due to various reasons including increase in traffic flow; increase in the allowable weight of vehicles compared with those considered in the initial design; harsh environmental conditions; use of deicing salts, especially in countries with cold climates; poor quality of construction materials; and limited maintenance. Many bridges in Europe suffer from the previously mentioned factors (PANTURA 2011), and the same is true for the United States in which ~~one third~~ of the 607,380 bridges are in need of maintenance (ASCE 2014). Bridge maintenance ensures serviceability along with safety for users and typically involves inspection, repair, strengthening, or replacement of the whole or part of a bridge. Such operations result in direct economic losses (e.g., material and labor costs) as well as indirect socioeconomic losses due to disruption of traffic flow, such as travel delays, longer travel distances, insufficient movement of goods, and business interruption. Depending on the type of bridge and the scale of the maintenance operations, indirect losses might be several times higher than direct losses and constitute one of the major challenges for bridge owners, decision makers, and bridge engineers (PANTURA 2011). Thus, sustainable methods for bridge repair, strengthening, or replacement that minimize direct costs and traffic flow disturbance are urgently needed.

Bridge decks typically deteriorate faster than other bridge components, e.g., the decks of ~~33%~~ of the bridges in America are in need of repair or replacement after an average service life of 40 years (ASCE 2014). It is important to note that deck replacement is the typical maintenance decision because repair methods, such as deck overlay, are not sufficient for long extension of the bridge life span (Deng et al. 2016). In the case of steel-concrete composite bridges, removing and replacing their deteriorating deck is a challenging process due to the connection among the deck and the steel beams. Such a connection is traditionally achieved with the aid of shear studs, which are welded on the top flange of the steel beams and are fully embedded within the concrete deck. Therefore, removing the deck involves drilling and crushing the concrete around the shear studs and then breaking the deck into manageable sections (Tadros and Baishya 1998). Such processes are costly and time-consuming and involve the use of hazardous equipment. Other bridge deterioration mechanisms include fatigue or corrosion in the steel beam or in the shear studs. Repair in these cases is again challenging and often questionable in terms of the postrepair structural integrity, whereas replacement of a deteriorating steel beam or shear stud is costly and time-consuming due to the previously mentioned monolithic connection between the steel beam, shear connectors, and concrete deck.

Apart from repairing or strengthening existing bridges, bridge engineers should adopt reparability and easy maintenance as major goals for new bridge design projects. This can be achieved not only by designing bridges based on a lifecycle cost approach that will assess repair costs and losses during their life span but also by changing the paradigm in structural detailing so that bridge structural systems have the inherent potential to be easily repaired, strengthened, or replaced. A possible way to meet this challenging goal is the development and design of novel bridge structural systems that allow bridge disassembly without compromising their structural integrity and efficiency. Rapid bridge disassembly will

[1]Ph.D. Candidate, School of Engineering, Univ. of Warwick, CV4 7AL, U.K.; Lecturer, Univ. of Baghdad, Baghdad 10071, Iraq (corresponding author). E-mail: ahmed.suwaed@outlook.com

[2]Professor of Structures and Structural Mechanics, Faculty of Engineering and the Environment, Univ. of Southampton, Southampton SO17 1BJ, U.K. E-mail: T.Karavasilis@soton.ac.uk

Note. This manuscript was submitted on August 15, 2016; approved on March 8, 2017; published online on [redacted]. Discussion period open until [redacted]; separate discussions must be submitted for individual papers. This paper is part of the ***Journal of Bridge Engineering***, © ASCE, ISSN 1084-0702.

offer the unique advantage of easy replacement of deteriorating structural components; therefore, it will result in the extension of bridge life span with minimum cost and traffic disturbance. In the case of steel-concrete composite bridges, bridge disassembly calls for a demountable shear connector that would allow easy separation of the deck from the steel beam without compromising composite action. The potential for bridge disassembly can be further facilitated by using precast concrete panels that are connected to each other with dry joints, such as those proposed by Hallmark (2012).

Background

Few works developed demountable shear connectors for steel-concrete composite beams. Dallam (1968), Dallam and Harpster (1968), and Marshall et al. (1971) performed tests to investigate the effect of pretensioning on the structural performance of high-strength friction-grip bolts used as shear connectors. A series of tests was conducted on three types of postinstalled bolted shear connectors by Kwon et al. (2010) and showed fatigue strength higher than that of welded studs. Kwon et al. (2011) also tested five full-scale beams using postinstalled bolted shear connectors and showed the effectiveness of such a strengthening strategy for noncomposite bridge girders. Pavlović et al. (2013) investigated the use of bolts as shear connectors and found adequate strength but low initial stiffness, i.e., 50% of that of welded shear studs. Moynihan and Allwood (2014) conducted three composite beam tests using bolts as shear connectors and found performance similar to that of welded shear studs. Dai et al. (2015) performed a series of push-off tests using bolted connectors machined from studs and found a large slip capacity along with shear resistance equal to 84% of that of welded studs at slip displacement equal to 6 mm. Ban et al. (2015), Pathirana et al. (2015), Henderson et al. (2015a), Henderson et al. (2015b), and Pathirana et al. (2016) investigated the behavior of composite beams using blind bolts as shear connectors and found that blind bolts achieve composite action similar to welded studs. Moreover, their research findings imply that blind bolts are beneficial to the time-dependent behavior of composite beams under sustained loads. Liu et al. (2014) investigated the behavior of high-strength friction-grip bolts as shear connectors for composite beams with geopolymer precast concrete slabs and identified three distinct regions in the load-slip behavior along with significant ultimate shear resistance and large slip capacity. Ataei et al. (2016) assessed the behavior of composite beams using the shear connector proposed by Liu et al. (2014). Their results showed significant initial stiffness due to pretensioning along with ductility higher than that of welded shear studs.

All the previous tests on friction-grip bolts as shear connectors revealed an undesirable large slip displacement due to bolts sliding inside the bolt holes when friction resistance in the steel beam-concrete slab interface was exceeded. It should be noted that the prestandard of Eurocode 4 (BSI 1994) included friction-grip bolts as shear connectors but with major restrictions in the exploitation of their full shear resistance. In particular, the BSI (1994) prestandard allowed the summation of two horizontal shear force resisting mechanisms (i.e., friction in the steel beam-concrete slab interface and shear force resisted by the bolt only) provided that the shear force-slip displacement behavior has been verified by testing. Moreover, Johnson and Buckby (1986) discussed the use of friction-bolts as shear connectors within the framework of the BS5400-5 (BSI 1979) standard for bridges. They mention that the shear resistance of friction-bolts should be assumed equal to friction resistance only, unless all the gaps among the bolt and the precast slabs are grouted after bolt tightening so that bearing of the bolt onto the precast slab will take place immediately after the initiation of slip in the friction interface.

Apart from the bolt sliding issue discussed in the previous paragraph, all the previously proposed bolted shear connectors may not be suitable for precast construction due to different practical reasons. In the case of shear connectors that are pre-embedded in the concrete slab, precast construction tolerances make their alignment with the predrilled bolt holes on the top flange of the steel beam extremely difficult, if not impossible. In the case of shear connectors that are fastened underneath the steel beam after positioning of the precast slab on the top of the steel beam, gaps in the concrete slab-steel flange interface may prevent adequate bolt fastening and cause slab cracking (Biswas 1986). Moreover, working underneath the bridge to fasten the bolts is time-consuming and is generally considered as a substandard unfavorable practice. It is also noted that connectors that are fully embedded within the concrete slab allow uplift and replacement of the slab as a whole but not full disassembly of the composite beam, i.e., replacement of the shear connectors in case of damage due to fatigue or corrosion is not possible.

This paper presents a novel demountable shear connector for precast steel-concrete composite bridges that overcomes all the issues mentioned in the previous two paragraphs. The connector

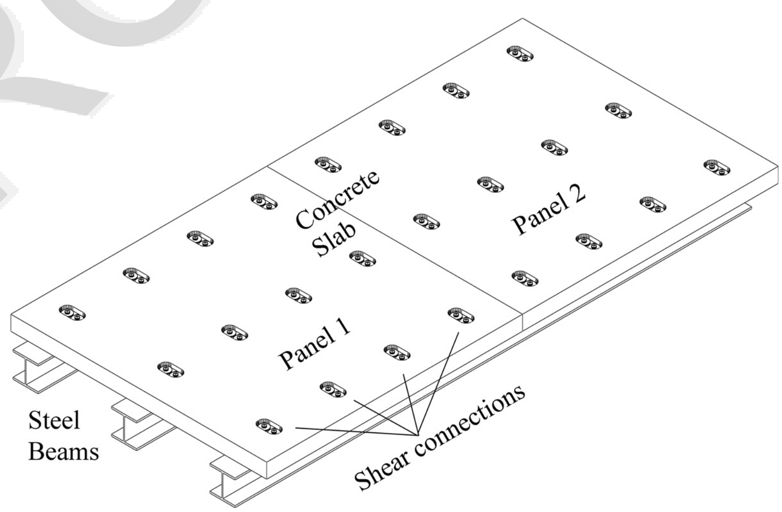

Fig. 1. Precast steel-concrete composite bridge using the novel shear connector

uses high-strength steel bolts, which are fastened to the steel beam with the aid of a special locking nut configuration that prevents bolts slipping within their holes. Additional structural details promote accelerated construction and ensure that the connector overcomes typical construction tolerance issues of precast structures. The connector allows full bridge disassembly. Therefore, it can address different bridge deterioration scenarios with minimum disturbance to traffic flow: (1) precast deck panels can be rapidly uplifted and replaced; (2) connectors can be rapidly removed and replaced; and (3) steel beams can be easily replaced, whereas precast decks and shear connectors can be reused. A series of push-out tests are conducted to assess the behavior of the connector and quantify the effect of important parameters. The experimental results show shear resistance, stiffness, and slip capacity higher than those of welded shear studs along with superior stiffness and strength against slab uplift. Identical tests reveal negligible scatter in the shear load-slip displacement behavior. A design equation is proposed to predict the shear resistance with absolute error less than 8%.

Novel Demountable Shear Connector

The proposed locking nut shear connector (LNSC) is one of the two demountable shear connectors invented by Suwaed et al. (2016).

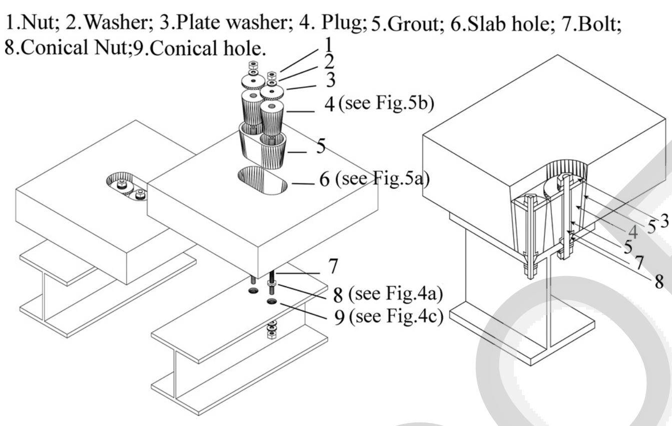

F2 : 1

Fig. 2. The 3D disassembly and inside view of the shear connector

Fig. 1 shows a steel-concrete composite bridge, which consists of precast concrete panels connected to steel beams with the aid of a LNSC. The concrete panels have several holes (pockets) to accommodate the shear connectors. Fig. 2 shows a three-dimensional (3D) disassembly along with an inside 3D view of the shear connector in which all its components are indicated. Moreover, Fig. 3 shows the cross section of a steel-concrete composite beam using the shear connector. The following paragraphs describe in detail the components of the LNSC and the associated methods of fabrication and construction.

The LNSC consists of a pair of high-strength steel bolts (e.g., Grade 8.8 or higher) with a standard diameter ~~(e.g., M16)~~, as shown in Fig. 3. These bolts are fastened to the top flange of the beam using a double nut configuration, which consists of a standard lower hexagonal nut (Nut 1 in Fig. 3) and an upper conical nut (Nut 2 in Fig. 3). The upper part of the bolt hole is a countersunk seat with chamfered sides following an angle of 60°, as shown in Fig. 4(c). The upper conical nut [Figs. 4(a and b)] is a standard type nut (BSI 1970) threaded over the bolt and has a geometry that follows the same 60° angle so that it can perfectly fit within the countersunk seat. ~~The upper conical nut locks within the countersunk seat, preventing slip of the bolt within the bolt hole.~~ A few millimeters of the total height of the upper conical nut appear above the top surface of the beam flange (Fig. 3) to resemble the height of the collar of welded shear studs (Oehlers 1980). In that way, the LNSC increases the contact area of the bolt with the surrounding concrete, which delays concrete crushing. Moreover, 5 mm of the internal threading of the conical nut is removed, as shown in Fig. 4(b). In that way, the bolt is partially hidden inside the conical nut and shear failure within its weak threaded length (as seen in other types of bolt shear connectors) is prevented. The lower standard hexagonal nut (BSI 2005c) is used along with a hardened chamfered washer (BSI 2005d) and a direct tension indicator (DTI) washer (BSI 2009a), as shown in Figs. 2 and 3. A proof load [e.g., 88–106 kN for an M16 bolt, which represents 70% of its ultimate capacity according to BSI (2009a)] is applied between the lower nut and the conical nut to ensure a robust locking configuration that prevents the bolt from slipping within its hole.

The slab pocket is a countersunk hole with an inclination of 5° following the recommendations of Vayas and Iliopoulos (2014). A typical geometry of a slab pocket, relevant to the test specimens

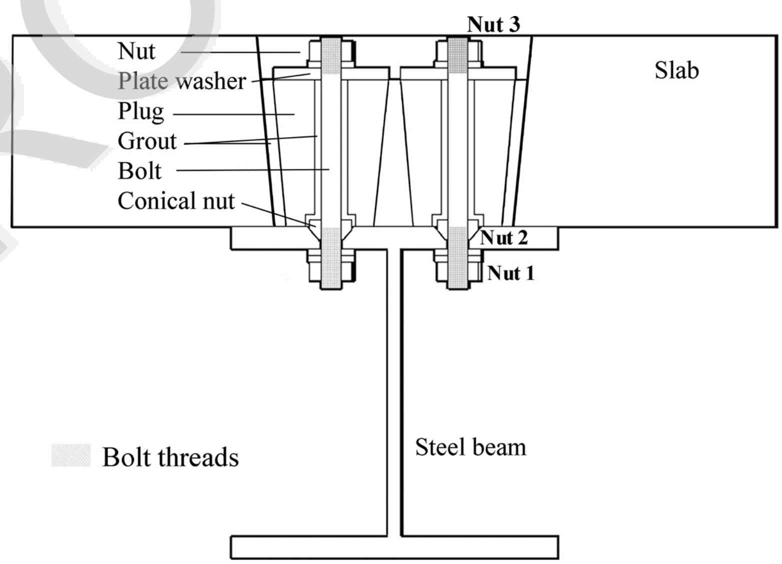

F3 : 1

Fig. 3. Cross section of a steel-concrete composite beam using the shear connector

presented later, is shown in Fig. 5(a). Inside each slab pocket there are two inverted conical precast concrete plugs (Figs. 2 and 3) with geometry following the inclination angle of the slab pocket. A typical geometry of a plug, relevant to the test specimens presented later, is shown in Fig. 5(b). Each plug has a central circular hole with a 26-mmm diameter that accommodates an M16 bolt with 10-mm clearance. The diameter of the central circular hole increases from 26 to 40 mm at the base of the plug to accommodate an M16 conical nut with 10-mm clearance, as shown in Fig. 5(b). The dimensions of the plug ensure that shear forces are transmitted from the LNSC to the concrete slab without the risk of premature longitudinal shear failure and/or splitting of the concrete slab. Moreover, the diameters of the plugs are small enough compared with the diameters of the slab pocket to overcome construction tolerance issues typically encountered during precast bridge construction (Hallmark 2012). Grout is used to fill the gaps between the bolt and the hole of the plug as well as the gaps between the plugs and the slab pocket (Figs. 2 and 3). Rapid hardening grout of ordinary strength that flows into gaps without bleeding or segregation is recommended for the LNSC. The height of the plug is 115 mm (i.e., less than the 150-mm height of the slab) to allow for additional cover or waterproof grout.

Fig. 3 shows that a hardened plate washer is used to uniformly distribute the bolt thrust on the upper face of the concrete plug without inducing cracks. The plate washer has a diameter of 90 mm, a central hole with an 18-mm diameter, and a 10-mm thickness. Tightening of Nut 3 (Fig. 3) is performed before hardening of the grout to avoid developing internal stresses in the slab. This way bolt tightening does not result in cracking of the slab due to imperfections in the steel beam-concrete slab interface (Badie and Tadros 2008).

It should be mentioned that different configurations of the LNSC could be adopted by using different numbers of bolts. For example, one bolt in one precast concrete plug within a single slab pocket can be adopted to reduce the quantity of in situ grout or four bolts in a single plug within a single slab pocket could be adopted to increase the total shear strength, reducing the shear connectors needed along the length of the bridge.

Procedure for Accelerated Bridge Assembly

Prefabrication of all structural components can be performed in the shop (i.e., machining of the conical nuts, drilling of the chamfered holes, positioning of the bolts on the steel beams by fastening the double locking nut configuration, casting of precast concrete plugs, and casting of precast slabs), whereas the final assembly between the precast slab and the steel beam is performed on-site. Each precast concrete panel is positioned on the top of the steel beam so that each pair of bolts is approximately aligned with the center of the slab pocket. Quick-hardening grout is then poured into the slab pocket up to a certain depth. Then, the plugs are placed into the slab pocket so that each plug surrounds a bolt and all gaps are filled with grout. The plugs are then secured in place by tightening Nut 3 in Fig. 3. Hardening of the grout completes the construction process of the LNSC.

Procedure for Accelerated Bridge Disassembly

The LNSC allows rapid disassembly and replacement of any deteriorating structural component of a precast steel-concrete composite bridge.

In case of deterioration in a precast concrete panel, the lower nuts (Nut 1 in Fig. 3) are removed and the precast panel along with

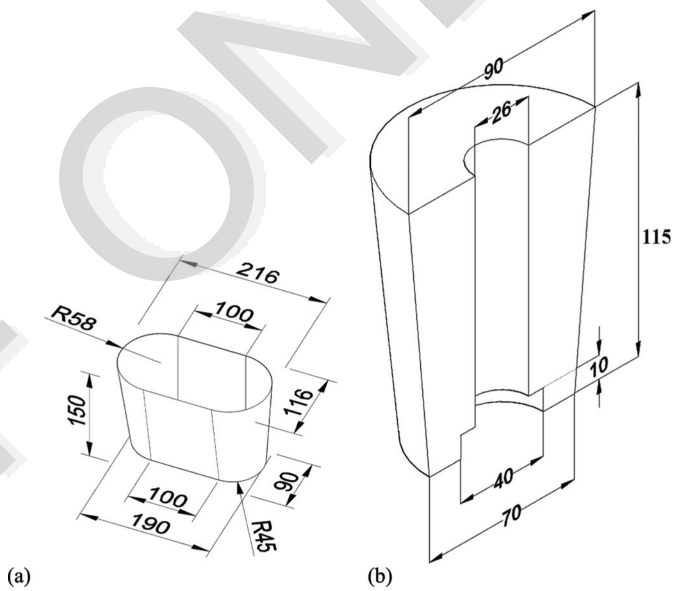

Fig. 5. Dimensions of (a) slab pocket and (b) half plug

F5 : 1

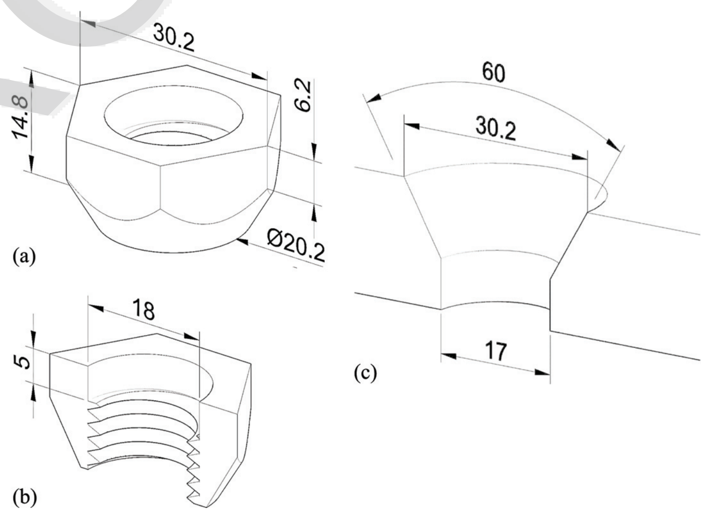

F4 : 1

Fig. 4. Geometry of the locking connection: (a) full nut; (b) half nut; (c) half countersunk hole

its shear connectors can be rapidly uplifted as a whole. If there is no access underneath the bridge, the upper nuts at the top of the plugs (Nut 3 in Fig. 3) are removed and the precast panel can be rapidly uplifted along with its plugs by leaving the bolts in place. To achieve that easily, it is important to design the bolts so that their threaded length is not in contact with the grout.

In case of deterioration in a few shear connectors, the plugs along with their surrounding grout can be rapidly extracted (pulled out) and replaced, as shown in Fig. 6 [i.e., first the lower nuts (Nut 1 in Fig. 3) are unfastened and then the plugs and their surrounding grout are removed by applying uplift forces while using the slab as support]. Optionally, a thin layer of a release agent like a wax-based material can be applied on the surfaces of the slab pocket before casting the grout to allow easier removal of the plugs and their surrounding grout.

In case of deterioration in the steel beam, the accelerated bridge disassembly capability allows the beams to be replaced, and the precast concrete panels and shear connectors can be reused. It is emphasized that robust dry joints among the precast concrete panels, such as those proposed by Hallmark (2012), would further enhance bridge disassembly.

Experimental Program

Test Setup and Instrumentation

Push-out tests on the LNSC were conducted using the test setup shown in Fig. 7. The specimen consists of a pair of slabs connected to a steel beam by using the LNSC. Both the specimen and the test setup follow the recommendations of Eurocode 4 (BSI 2004). A hydraulic jack with ~~the~~ capacity of 200 tons was used to apply a vertical force on the specimen. Four LVDTs were used to measure slip between the concrete slabs and the steel beam close to the positions

F6 : 1 **Fig. 6.** Disassembly procedure

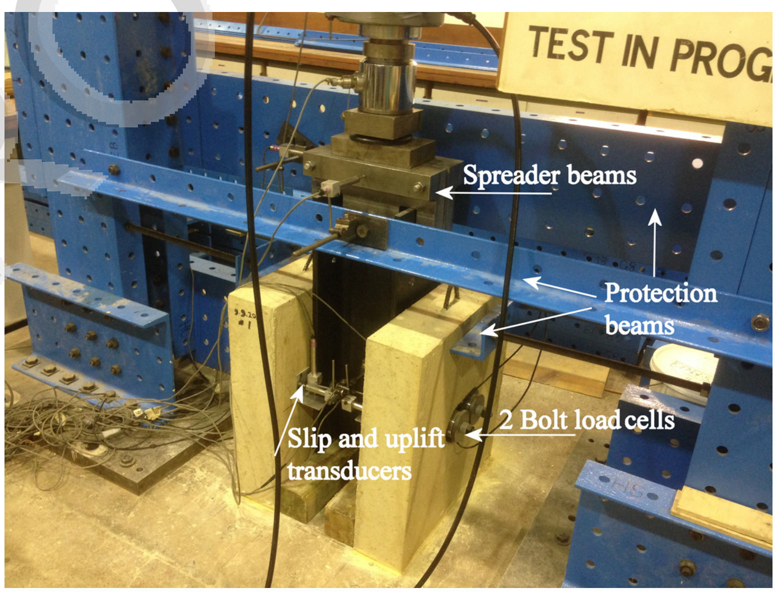

F7 : 1 **Fig. 7.** Setup for push-out tests and instrumentation of the four bolts. Another pair of LVDTs was used to measure lateral displacements at the upper tip of the specimen so that any eccentricity in the loading could be detected in advance. Moreover, four LVDTs were used to measure separation (i.e., uplift displacements) of the concrete slabs from the steel beam close to the positions of the four bolts. An additional LVDT was used to monitor the jack displacement and to control the displacement rate during testing. A load cell with a capacity of 100 tons was used to measure the applied load directly under the jack. The load is transferred through a ball joint that ensures that the line of action of the load passes exactly through the centroid of the steel section without any eccentricity. This point load is uniformly distributed to the two flanges of the steel beam with the aid of two spreader beams, which are connected together by four bolts parallel to the steel section flanges. The internal loads in the bolts of the LNSC were measured with the aid of washer load cells with a 200-kN capacity, which were positioned between two plate washers and then secured by a nut above each concrete plug. The push-out tests were performed under a load control of 40–60 kN/min during the initial linear shear load-slip displacement behavior phase, and then under a displacement control of 0.1–0.2 mm/min during the subsequent nonlinear shear load-slip displacement behavior phase.

Specimens and Materials Properties

The steel beam has a length equal to 80 cm, a 254 × 254 × 89 UC section, and S355 steel grade. Four holes with countersunk seat upper parts [exact dimensions for the case of M16 bolts are shown in Fig. 4(c)] were drilled on the beam flanges. Four bolts (threaded at both ends) and four compatible conical nuts [exact dimensions for the case of M16 bolts are shown in Figs. 4(a and b)] were fabricated. The bolts along with their conical nuts were inserted into the countersunk seat holes of the steel beam. Then, the lower nuts (Nut 1 in Fig. 3) were tightened to the proof load to securely lock the bolts within the bolt holes. A DTI washer was used to confirm the proof load limit for each bolt. Fig. 8 shows the bolts and the conical nuts securely locked within the chamfered holes of the steel beam.

The precast concrete slab had a 650 × 600 × 150-mm geometry and a central countersunk conical pocket with the exact dimensions shown in Fig. 5(a). The slab pocket was treated with two layers of a release agent (Pieri Cire LM-33) from Grace Construction Products. The slab steel reinforcement was designed according to Eurocode 4 (BSI 2004). Slabs were cast in horizontal position and

Fig. 8. Bolts and conical nuts ~~securely~~ locked within the chamfered holes of the beam flange

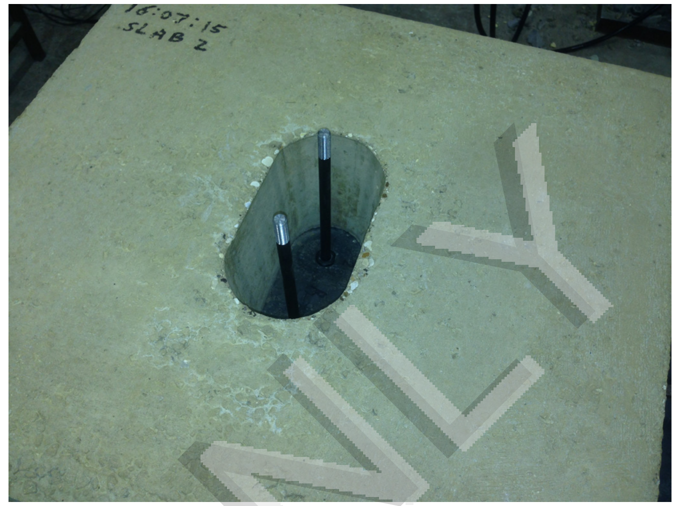

Fig. 9. Slab positioned over the steel beam

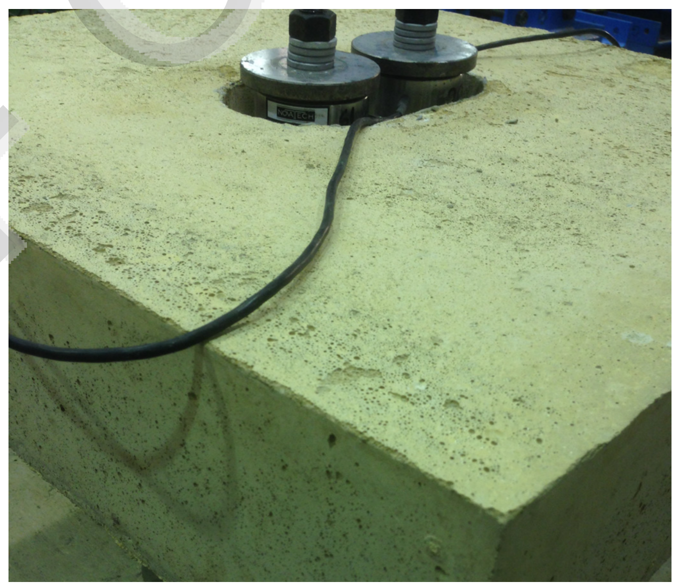

Fig. 10. Nut and washer load cell on top of the concrete plugs

Table 1. Typical Mix Proportions for Slabs, Plugs, and Grout

Material	Slabs (kg/m^3)	Plugs (kg/m^3)	Grout (kg/m^3)
Cement	313	500	910
Cement type	CEM II A-L 32.5 R	CEM I 52.5N	Hanson Quickcem
Water	189	182	455
Sand	825	713	910 fine sand
Gravel	1,093 (size 10 mm)	1,011 (size 10 mm)	—
Superplasticizer	0.8% of cement weight	1.2% of cement weight	—

Table 2. Specifications of Push-Out Tests

Test number	Bolt diameter (mm)	Bolt preloads (kN) Nuts 1–2[a]	Bolt preloads (kN) Nuts 2–3[a]	Slabs Composite strength (MPa)	Slabs Tensile strength (MPa)	Plugs Composite strength (MPa)	Plugs Tensile strength (MPa)	Grout Composite strength (MPa)
1	16	88–106	88–106	31	2.5	65	4.2	122
2	16		0.0					
3	16	88–106	88–106	31	2.5	65	4.2	—
4	16	88–106	10	31	2.5	83	5.2	43
5	16	88–106	88–106	37	—	71	4.3	58
6	16	64	55–70	41	4.0	86	5.1	44
7	12	47–56	24	50	4.0	91	4.8	28
8	14	68–81	23	50	4.0	95	4.6	32
9	16	Failed	23	42	3.6	80	4.8	39
10	16	88–106	24	43	3.1	50	3.7	27
11	16	88–106	26	43	3.2	96	4.8	28
12	16	88–106	26	42	3.5	91	4.9	28

[a]See Fig. 3 for locations of Nuts 1–3.

Table 3. Sieve Analysis of Fine Sand Used in Grouts

Sieve size (mm)	Cumulative (% by weight)	Passing (% by weight)	BSI (1976), Table 1, Type B, passing (% by weight)
0.6	0	100	55–100
0.3	34	66	5–75
0.15	58	8	0–20
0.063	8	0	<5

then positioned over each flange of the steel beam, as shown in Fig. 9. Grout was poured into the slab pockets, and then a precast plug [with the exact dimensions shown in Fig. 5(b)] was placed around each bolt and gradually inserted into the slab pocket to ensure that all gaps were filled with grout without leaving any voids.

A washer load cell was placed between two plate washers on the top surface of each plug to measure the tension load inside the bolts, as shown in Fig. 10. Tightening the nut above each plug (Nut 3 in Fig. 3) completed the fabrication of the LNSC specimen. All bolts had approximately the same tension force after tightening all nuts above the plugs to ensure symmetrical behavior of the specimen.

Typical mix proportions used to cast concrete slabs, plugs, and grout are listed in Table 1. Moreover, Table 2 lists specifications for all push-out tests (discussed in the next section) including concrete compressive and tensile strengths obtained at the same day of each push-out test. The maximum size of the gravel was 10 mm. The sieve analysis (BSI 1976) for the "fine" sand used for the grout is provided in Table 3. It is important to use such fine sand and not an ordinary sand to avoid possible segregation of sand particles between the lower face of the plug and the upper face of the steel flange. The compressive strengths of the slabs and plugs were evaluated by using standard cubes of a 100-mm length, the compressive strength of the grout by using cubes of a 75-mm length, and the tensile strengths of the slabs and plugs by using standard cylinders of a 100-mm diameter and 200-mm length.

Nine steel coupon specimens, randomly chosen and machined from bolts, were subjected to tensile tests according to BSI (2009b). Specimen strains were measured using an axial extensometer. Average values of the properties of the steel bolts are listed in Table 4, whereas a typical stress-strain relationship from one coupon test is shown in Fig. 11.

Table 4. Properties of Bolts

Test	Modulus of elasticity (GPa)	Yield stress (MPa)	Tensile strength (MPa)	Maximum elongation %	Bolt tensile resistance (kN)
Average of nine specimens	209	787	889	8	—
Min.	201	719	832	5	—
Max.	215	847	950	15	
Standard deviation	5	50	41	5	
D12 mm	—	—	—	—	100.5
D14 mm	—	—	—	—	136.9
D16 mm	—	—	—	—	178.7

Experimental Results

Preliminary Tests

Push-out tests were performed on 12 LNSC specimens with specifications listed in Table 2. The first six tests were preliminary and served to investigate how different design details influence the strength and ductility of the LNSC. The results of these preliminary tests led to the recommendation of the final robust structural details of the LNSC. The specimens of Tests 1 and 2 used very high strength grout, a double nut configuration similar to the work of Pavlović et al. (2013), and two bolts per plug. These tests showed early shear failure in the threaded part of the bolts and modest slip capacity. The specimen of Test 3 used two bolts per plug and a gap between the bolt and its hole [i.e., similar to the work of Liu et al. (2014)] with an extra enlargement at the bolt base equal to 20 mm. Test 3 showed failure due to excessive slip, which was similar to the failure discussed by Oehlers and Bradford (1999). The specimen of Test 4 was identical to that of Test 3, but the gap between the bolt and its hole was filled with a cement-based grout. Test 4 showed shear failure in the threaded part of the bolt. During the previously mentioned four tests, a sudden and large slip occurred as a result of bolts sliding inside the bolt holes when friction resistance in the steel beam-concrete slab interface was exceeded. To this end, Test 5 aimed to assess the behavior of a nonslip shear connector using a conical nut connection similar to that of the LNSC but without completely hiding the threads of the bolt inside the conical nut body, as shown in Fig. 12 (refer to Fig. 8 for comparison). Finally, Test 6 was conducted on a specimen representing the actual robust structural details of the LNSC. Fig. 13 compares the shear load-slip displacement behavior from Tests 1 to 6 and highlights that the novel structural details of the LNSC result in superior structural performance. In Fig. 13 (as well as in all the shear load-slip displacement curves presented in this paper), the shear load is the applied load divided by four (i.e., number of bolts), whereas the slip displacement is the average of the slip displacements measured close to the four bolts. The ultimate load is the maximum load in the shear load-slip displacement curve, whereas the slip capacity is calculated as the slip displacement corresponding to the ultimate load. It should be noted that Eurocode 4 (BSI 2004) ~~recommended~~ calculating the slip capacity as the one that corresponds to the characteristic load value in the descending branch of the shear load-slip displacement curve. However, to accurately record the descending branch of a push-out test, a very stiff testing rig that does not store high strain energy at the instant of ultimate load (i.e., instant of sudden failure) is required (Johnson 1967).

Confirmation of Results with Identical Tests

Following the recommendation of Eurocode 4 (BSI 2004), the results of Test 6 were confirmed by conducting two additional push-out tests with approximately the same specifications (i.e., Tests 11 and 12 in Table 2). Table 5 lists the ultimate loads and slip capacities from the "identical" Tests 6, 11, and 12. The deviation of the ultimate load of any of the individual tests from the mean value is less than 2%, i.e., significantly below the 10% limit of Eurocode 4 (BSI 2004). Therefore, the characteristic shear resistance may be safely determined as the minimum ultimate load from the three identical tests reduced by 10% according to Eurocode 4 (BSI 2004), i.e., $P_{Rk} = 0.9 \times 189.5 = 170.55$ kN. Fig. 14 compares the shear load-slip displacement behavior from the three identical push-out Tests 6, 11, and 12. The results highlight that the robust structural details of the LNSC result in superior strength, superior stiffness, large slip capacity, and repeatability in the load-slip behavior. Moreover, Suwaed et al. (2016) provided a comparison among the LNSC and previously proposed demountable shear connectors, which shows that the LNSC provides the highest shear resistance.

Comparison with Welded Studs

The shear resistance of the LNSC from Test 6 is equal to 198.1 kN for a slab concrete strength equal to 41 MPa, bolt diameter equal to 16 mm, and bolt tensile strength equal to 889 MPa. According to

Fig. 12. Bolts of the shear connector before and after ~~Test 5~~ F12 : 1

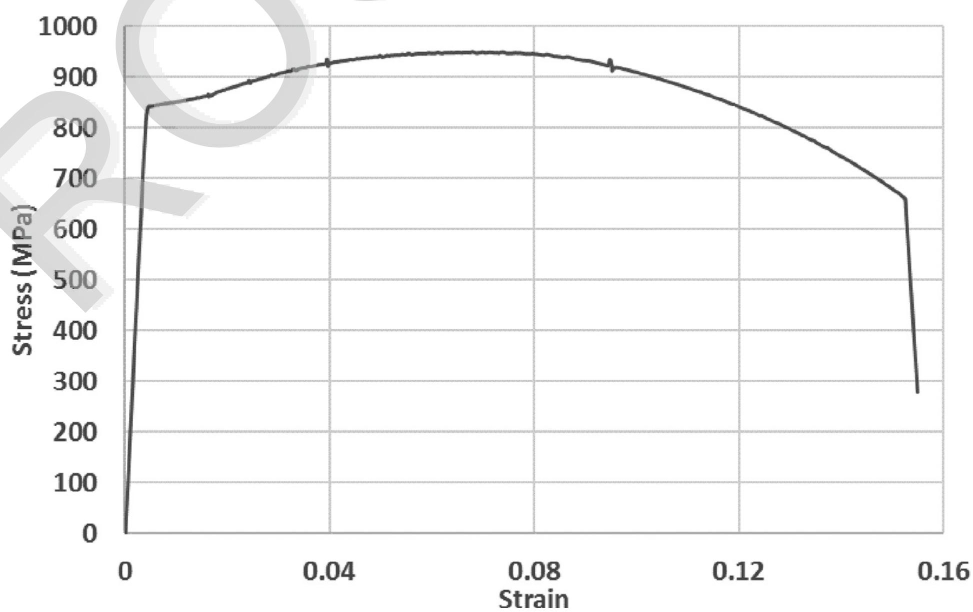

F11 : 1 **Fig. 11.** Typical stress-strain behavior of bolts from tensile coupon tests

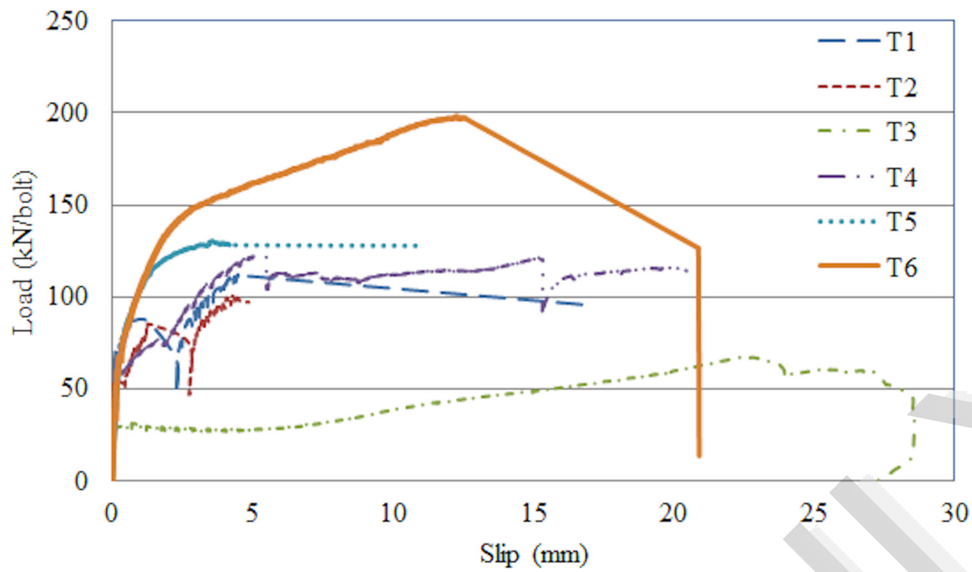

F13 : 1

Fig. 13. Comparison of load-slip behavior from ~~Tests 1 to 6~~

Table 5. Results of Tests 6, 11, and 12

Test number	Ultimate load (kN)	Slip capacity (mm)
6	198.1	12.2
11	196.7	13.9
12	189.5	13.8
Average	194.8	13.3
Standard deviation	3.76	0.779
Error %	2	6

Eurocode 4 (BSI 2004), the shear resistance of welded shear studs is calculated as the minimum of

$$P_R = 0.8\, f_u\, \pi \frac{d^2}{4} \tag{1}$$

and

$$P_R = 0.29\, d^2 \sqrt{f_{ck} E_{cm}} \tag{2}$$

where d = shank diameter of the welded stud; f_u = ultimate tensile strength of the steel material of the stud; f_{ck} = characteristic compressive cylinder strength of the concrete slab; and E_{cm} = elastic modulus of the concrete. By using the concrete slab strength, stud diameter, and tensile strength of the LNSC from Test 6 in Eqs. (1) and (2), the shear resistance of the corresponding welded shear stud is calculated equal to 73.02 kN from Eq. (2). Therefore, the shear resistance of the LNSC is significantly higher than that of welded studs. The reason for such higher shear resistance is that the smart structural details of the LNSC promote failure in the shank of a high tensile strength (e.g., 889 MPa) bolt without premature concrete failure, i.e., a behavior that is impossible for welded shear studs of similar high tensile strength. It should be noted that prior research shows negligible effect in the shear resistance of welded shear studs when high-strength grout (e.g., 75 MPa) is used to fill the pockets of the precast slab (Shim et al. 2001). Most importantly, although a tensile strength of 895 MPa was used for the welded shear stud in the previously mentioned calculations, Eurocode 4 did not allow the use of welded studs with tensile strengths higher than 500 MPa (BSI 2004); this is probably because welding steel structural elements of different steel grades (i.e., shear stud and steel beam) is not possible.

The slip capacity of the LNSC from Test 6 is equal to 12.2 mm, i.e., two times higher than the typical 6.0-mm slip capacity of welded studs. This large slip capacity of the LNSC could be exploited in the design of long composite beams on the basis of the partial interaction theory (Johnson and May 1975). The latter designs cannot be achieved with welded shear studs due to their limited slip displacement capacity (Johnson 1981).

The LNSC does not show appreciable scatter in its behavior (Fig. 14) compared with the scatter seen in the behavior of welded shear studs [e.g., see results in Xue et al. (2008)]. The main reason for this is that the smooth flowable grout used to cover all gaps among the elements of the LNSC ensures uniform distribution of bearing stresses in the conical nut-grout, bolt shank-grout, and plug-grout interfaces. Such uniform distribution of bearing stresses cannot be ensured in the area around the collar of welded shear studs due to the existence of voids and/or the variation in local arrangement of the aggregate particles (Johnson 2004).

Load-Slip Behavior and Failure Mode

The shear force transfer mechanism of the LNSC initiates with friction forces in the steel flange-concrete plug interface. The concrete plugs transfer these forces to the slab through the grout in their interface. When the shear forces exceed the friction resistance in the steel flange-concrete plug interface, slip occurs. Then, apart from friction, shear forces are also transferred from the steel flange to the conical nut and the bolt shank through bearing. The conical nut and bolt shank transfer forces to their surrounding grouts. Finally, these forces are transferred to the concrete plugs and then to the slab through the grout in their interfaces.

It should be noted that concrete is significantly stronger in triaxial compression, i.e., stresses can reach values equal to 10 times the cylinder strength (Johnson 1967). Oehlers and Bradford (1995) estimated that the concrete adjacent to the collar of a welded stud can withstand 7.0 times its cylinder strength. The part of the concrete plug in front of the conical nut is under nearly triaxial stress confinement conditions due to the pretensioning of Nut 3 in Fig. 3; therefore, it can develop stresses much higher than its 80- to 100-MPa design strength. Therefore, bolts will always shear off before the

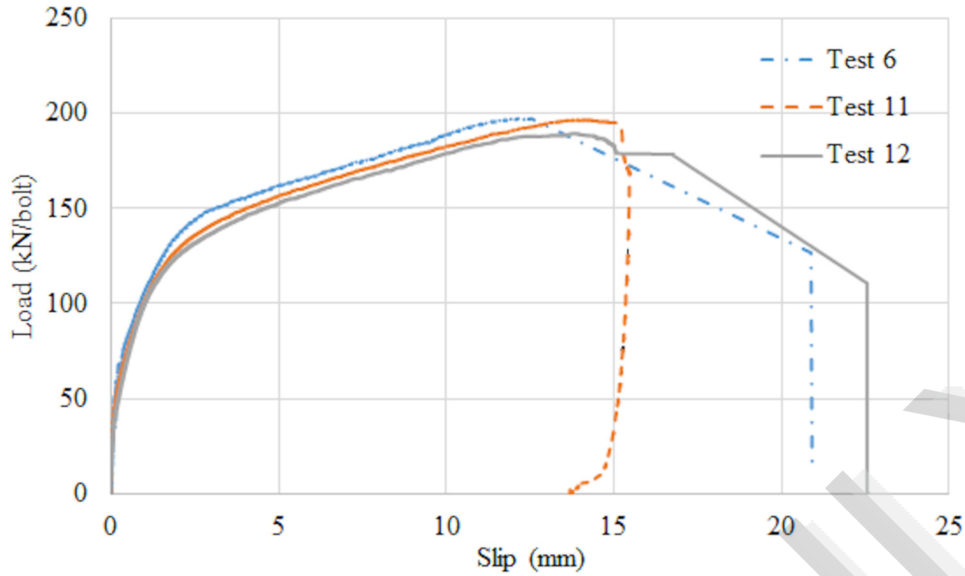

F14 : 1 **Fig. 14.** Behavior of shear connector from three identical push-out tests (6, 11, and 12 in Table 2)

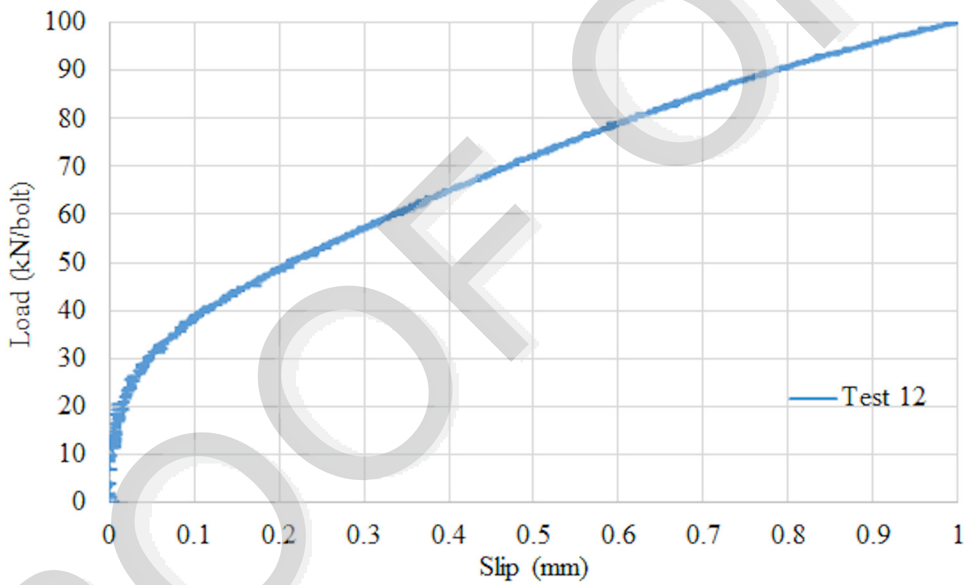

F15 : 1 **Fig. 15.** Results of Test 12 for slip displacement up to 1.0 mm

concrete plug fails. On the other hand, the existence of ordinary strength grout enables the bolts to deflect by crushing the grout in the plug-bolt interface. Such bolt deflection enables the LNSC to develop its large slip capacity.

The shear load-slip displacement behavior of the LNSC (Fig. 14) consists of three regions. The first region covers slip displacements from 0.0 to 1.0 mm in which the shear load reaches values up to 100 kN, i.e., approximately equal to 50% of the shear resistance, which means that the stiffness of the LNSC for the M16 bolt is 100 kN/mm. Similar stiffness can be offered by 19-mm-diameter welded studs according to Eurocode 4 (BSI 2004), which shows the superior stiffness of the LNSC. Fig. 15 plots the results of Test 12 for slip displacements up to 1.0 mm and shows that no slip occurs for shear loads lower than 12 kN. This initial nonslip behavior is due to friction within the steel flange-concrete plug interface. A friction resistance equal to 12 kN indicates a value of the friction coefficient equal to 0.5 [on the basis of the 26-kN bolt preload in Test 12 (Table 2)], which is ~~compatible~~ with the recommendation of BS 5400-5 (BSI 1979) for steel-concrete interfaces. Please note that bolt preloading is performed before grout hardening; therefore, 100% of the bolt preload is transferred as normal force in the steel flange-concrete plug interface. It should be mentioned that when the shear load exceeds the shear resistance, no sudden slip is seen in the behavior of the LNSC due to the locking nut configuration. Moreover, as the slip displacement increases, the length of the bolts increases and their internal forces slightly increase. The latter results in gradual increase of the friction resistance.

The second region of Fig. 14 covers slip displacements from 1.0 to 2.5 mm in which the shear load reaches values up to 130–150 kN, i.e., approximately equal to 75% of the shear resistance. In this

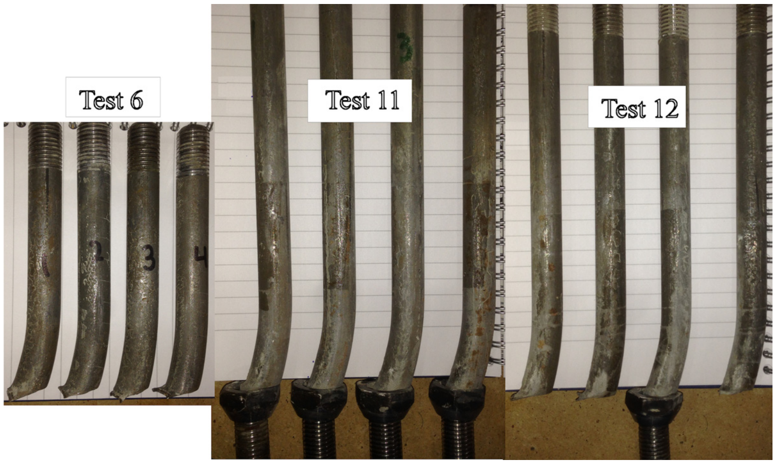

F16 : 1 **Fig. 16.** Deflected shapes of the bolts from push-out Tests 6, 11, and 12

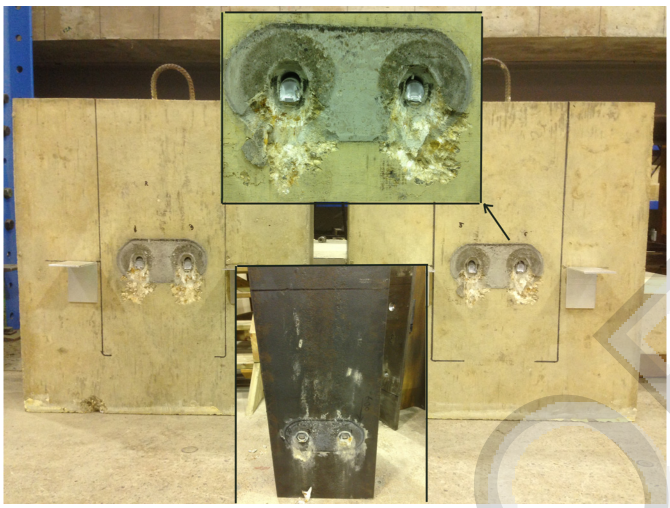

F17 : 1 **Fig. 17.** Slab spalling after push-out Test 6

region, gradual yielding of bolts in combined shear and bending along with crushing of the grout in front of the conical nut and the bolt shank take place. At the end of this region, the bolts form two short length regions of high plasticity (i.e., "plastic hinges" due to combined shear, bending, and axial internal stresses) separated by a 30- to 40-mm straight part.

The last region in Fig. 14 covers slip displacements from 2.5 mm to about 14 to 15 mm, in which the shear load reaches its 180- to 200-kN ultimate value. This region starts with the conical nut and bolt shank gradually bearing against the concrete plug. The latter action increases the concrete shear strains in the part of the plug that is in front of the conical nut. Then a concrete shear failure plane forms and passes through the grout-plug-grout-slab interfaces, starting just above the conical nut and ending just above the steel flange (slab spalling). The previously mentioned concrete shear failure shifts the bearing stresses from the locking nut to the bolt shank and finally leads to shear failure through an elliptical cross section of the bolt shank just above the conical nut (Fig. 16). It should be noted that deformations in the bolts of the LNSC are a combination of shear, bending, and tensile deformations. Similar behavior was observed in welded studs in which the combination was 56% bending deformations and 37% shear deformations (Pavlović et al. 2013). It should be noted that higher tensile deformations in shear studs could occur at specific locations of a bridge (e.g., close to transverse bracing) due to large tensile forces (Lin et al. 2014). ~~This case is explicitly addressed in Eurocode 4 (BSI 2005b), which recommended the use of additional anchorage mechanisms (e.g., steel plates welded on the top flange of the steel beam) (Vayas and Iliopoulos 2014) instead of designing the shear studs to resist such large tensile loads,~~ Also note that bolts subjected to combined shear and pretensioning do not necessarily exhibit reduction in their shear resistance. For example, Pavlović (2013) did not notice any influence on shear strength for preloading up to 100% of proof load. The latter also has been highlighted by Wallaert and Fisher (1964), in which it was explained that when a bolt is torqued to a certain preload, most of the inelastic deformations develop in the threaded portion of the bolt and not in the shank. Therefore, ~~the shear resistance is not decreased~~ when the failure plane is within the shank. It is interesting to note that spalling of the concrete slab was minor and without any global cracking or splitting in the LNSC tests (Fig. 17). The latter implies that in the case of the LNSC, and contrary to welded studs, there is no need for additional transverse reinforcement in the slab (BSI 2005b).

Load-Slab Uplift Behavior

During a standard push-out test (Oehlers and Bradford 1995), slabs tend to uplift as they slide over the collar of welded studs (Johnson 2012). Eurocode 4 (BSI 2004) and other researchers (Yam 1981) recommended that the slab uplift (i.e., slab separation) should be no more than 50% of the corresponding slip displacement for shear load equal to 80% of the shear resistance. Fig. 18 shows that slab separation is less than 0.1 mm at 80% of loading, i.e., only 4% of the corresponding slip displacement. Push-out tests on welded studs of the same bolt diameter showed uplift displacements equal to 9–15% of the corresponding slip displacements (Spremić et al. 2013).

Fig. 19 shows that the internal bolt force in the LNSC increases almost linearly with the slip displacement and finally reaches a value of 70–75 kN (i.e., 40% of the bolt tensile resistance) at the onset of failure. The angle of the line of action of this force from the vertical gradually increases as the slip displacement increases. Therefore, the internal bolt force has a vertical component that contributes to friction resistance and a horizontal component that directly contributes to shear resistance.

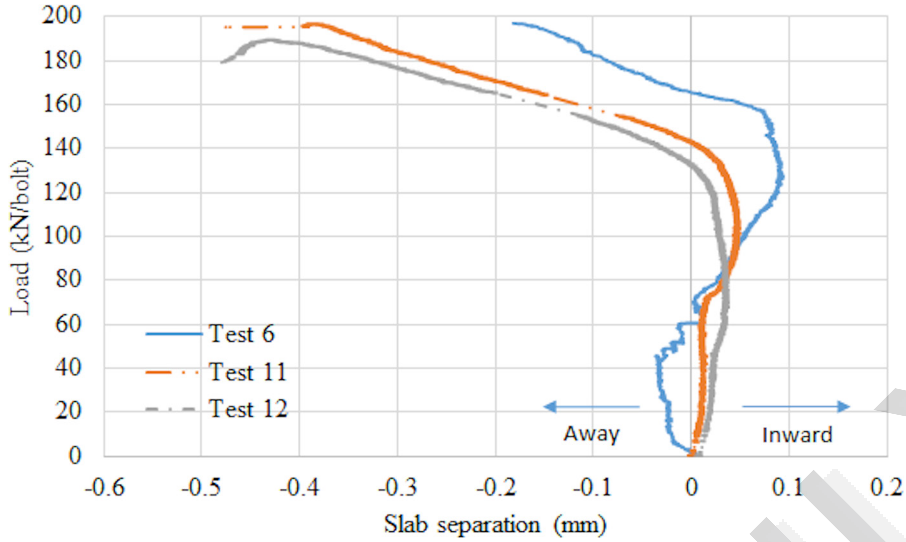

F18 : 1

Fig. 18. Comparison of slab separation from Tests 6, 11, and 12

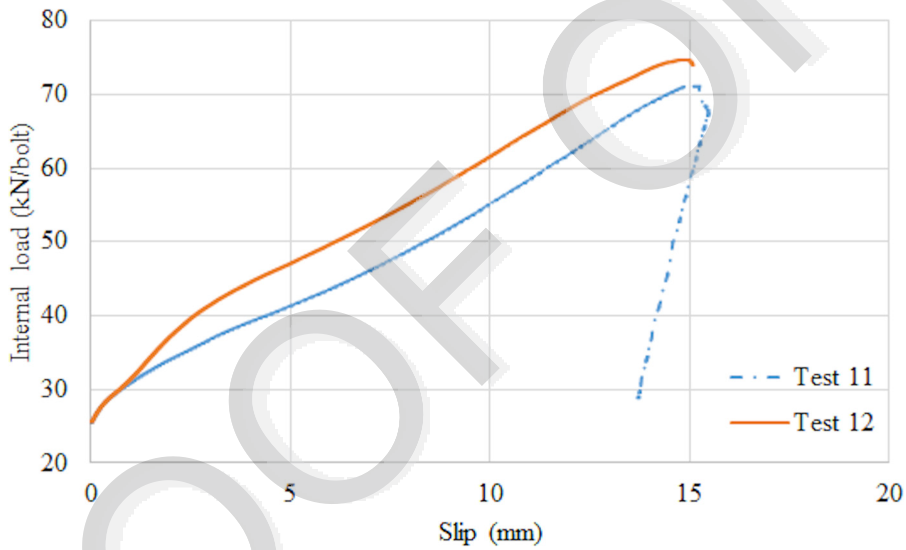

F19 : 1

Fig. 19. Bolt internal force from Tests 11 and 12

Table 6. Angle β of the Deflected Shape of the Bolt from the Vertical (in Degrees): M16 bolts of Tests 11 and 12

Test number	Bolt 1	Bolt 2	Bolt 3	Bolt 4	Average
11	12.9	12.1	12.1	9.7	11.7
12	11.3	11.3	13.7	13.7	12.5
Average	12.1	11.7	12.9	11.7	12.1

Design Equation

Eurocode 4 recommended that the shear resistance of a connector failing due to steel fracture can be calculated by using Eq. (1). In the case of the LNSC, Eq. (1) should be modified to account for the effect of friction in the steel flange-concrete plug interface, the effect of the inclination of the deflected shape of the bolts [similarly to the work of Chen et al. (2014)], and the effect of shear failure through an elliptical cross section of the bolt shank

$$P = 0.8 f_{\mathrm{u}} \left(\frac{\pi d^2}{4 \cos\beta} \right) + T(\sin\beta + \mu\ \cos\beta) \tag{3}$$

where β = angle of the deflected shape of the bolt from the vertical at the level of the shear failure plane; μ = coefficient of friction between concrete and steel; and T = tensile force in the bolts at the onset of failure. T was found equal to 40% of the bolt tensile resistance at the onset of failure (Fig. 19); therefore, after substitution and rearrangement Eq. (3) becomes

$$P = \frac{\pi d^2 f_u}{4} \left[\frac{0.8}{\cos\beta} + 0.4(\sin\beta + \mu\ \cos\beta) \right] \tag{4}$$

where for Tests 11 and 12, f_{u} = 889 MPa from Table 4; d = 16 mm from Table 2; μ = 0.5; and β = 12.1° from Fig. 16 and Table 6. Substitution of these values in Eq. (4) results in shear resistance equal to 196.2 kN, which is equal to the average shear resistance

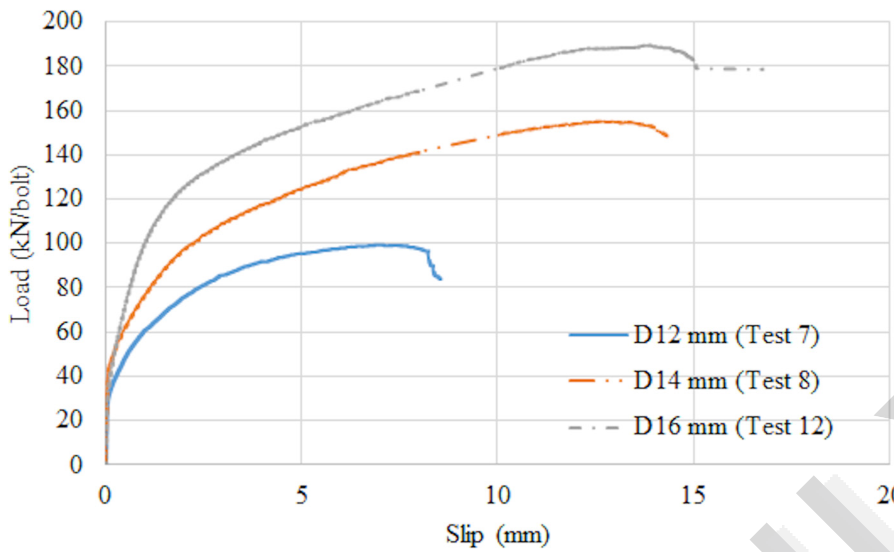

F20 : 1 **Fig. 20.** Effect of bolt diameter on the load-slip behavior

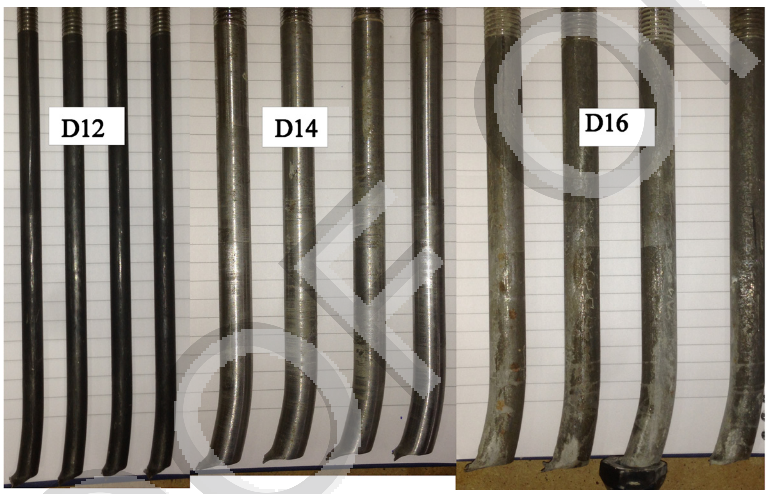

F21 : 1 **Fig. 21.** Deflected shapes of D12, D14, and D16 bolts from Tests 7, 8, and 12

Table 7. Results of Tests 7, 8, and 12

Test number	Bolt diameter (mm)	Collar height (mm)	Conical nut width (mm)	Ultimate load (kN)	Slip capacity (mm)	Ultimate load/bolt tensile resistance[a]	Bolt internal load/bolt tensile resistance[a]
7	12	2.5	23	99.3	7.0	0.99	0.34
8	14	5.0	27	155.2	12.9	1.1	0.35
12	16	6.0	29	189.5	13.8	1.1	0.45
Average	—	—	—	—	—	1.06	0.38
Standard deviation	—	—	—	—	—	0.0596	0.0497
Error %	—	—	—	—	—	6	13

[a]Bolt tensile resistance is provided in Table 4.

from push-out Tests 6, 11, and 12 in Table 5. It is interesting to note that by substituting $\mu = 0.5$ and $\beta = 12.1°$ into Eq. (4), the shear resistance of the LNSC becomes equal to 1.1 times the bolt tensile resistance. The latter value is significantly higher than the ~~pure~~ shear resistance of a bolt of the same diameter, i.e., 0.58 times the tensile resistance (BSI 2005a).

Experimental Parametric Studies

Effect of Bolt Diameter (Tests 7, 8, and 12)

Three bolt diameters, i.e., 12, 14, and 16 mm, were used in push-out Tests 7, 8, and 12 (Table 2) to explore the validity of Eq. (4). The shear load-slip displacement curves and the deflected shapes of the

Table 8. Angle β (in Degrees) and Length of Deflected Shape for M12, M14, and M16 Bolts

Bolt diameter (mm)	Bolt 1	Bolt 2	Bolt 3	Bolt 4	Average	Deflected length (mm)
12	7.7	9.9	8.5	9.9	9.0	28
14	10.5	11.3	11.3	12.1	11.3	35
16	11.3	11.3	13.7	13.7	12.5	40

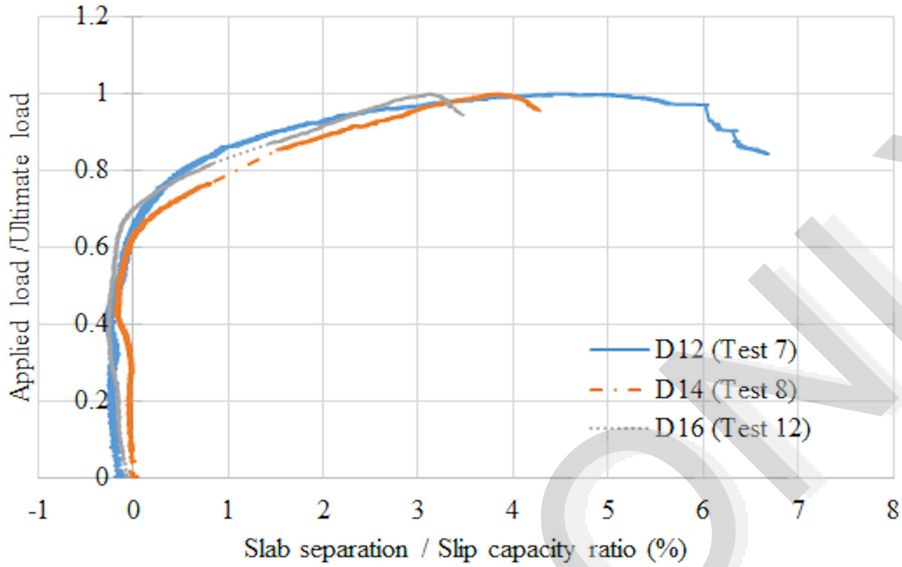

F22 : 1 **Fig. 22.** Effect of bolt diameter on slab uplift displacement

Table 9. Effect of Plug Concrete Strength on M16 Shear Connector Behavior

Test number	Bolt diameter (mm)	Plug strength (MPa)	Ultimate load (kN)	Slip capacity (mm)	Ultimate load/bolt tensile resistance[a]	β (degrees)
10	16	50	180.7	14.7	1.01	13.0
11	16	96	196.7	13.9	1.10	11.7
12	16	91	189.5	13.8	1.06	12.5

[a]Bolt tensile resistance is provided in Table 4.

bolts from these tests are shown in Figs. 20 and 21, respectively. Results of these tests are listed in Tables 7 and 8 and show that all connectors have large slip capacity (i.e. larger than the 6-mm limit of Eurocode 4) (BSI 2004). Moreover, the values of the seventh column in Table 7 confirm that the LNSC shear resistance can be approximately obtained as 1.1 times the bolt tensile resistance.

Substituting appropriate values for the M14 bolt into Eq. (4) results in shear resistance equal to 149.2 kN, which is only 4% lower than the corresponding value in Table 7. Similarly, Eq. (4) provides a shear resistance equal to 107.6 kN for the M12 bolt, which is only 8% higher than the corresponding value in Table 7. The earlier results show that Eq. (4) reliably predicts the resistance of the LNSC for three different bolt diameters.

Fig. 22 shows the effect of bolt diameter on slab uplift displacement in which the vertical axis represents the ratio of the applied load to the shear resistance, whereas the horizontal axis represents the ratio of the uplift displacement to the slip capacity. It is interesting to note that no uplift occurs for loads up to 60–70% of the shear resistance. Furthermore, at the onset of failure, the uplift displacements are equal to only 3, 4, and 5% of the corresponding slip displacements for M16, M14, and M12 bolts, respectively.

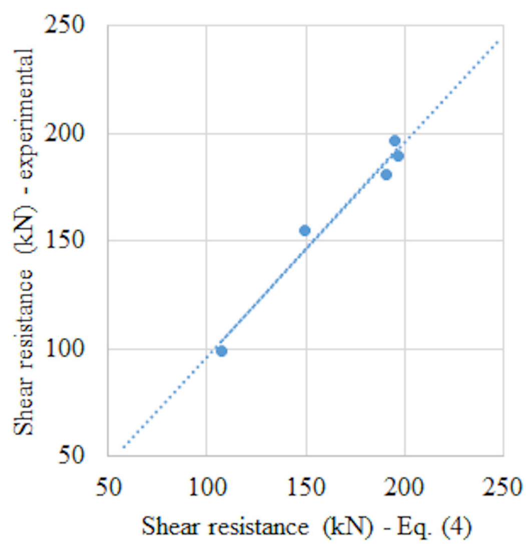

Fig. 23. Comparison between the predictions of Eq. (4) and the push-out tests results F23 : 1 F23 : 2

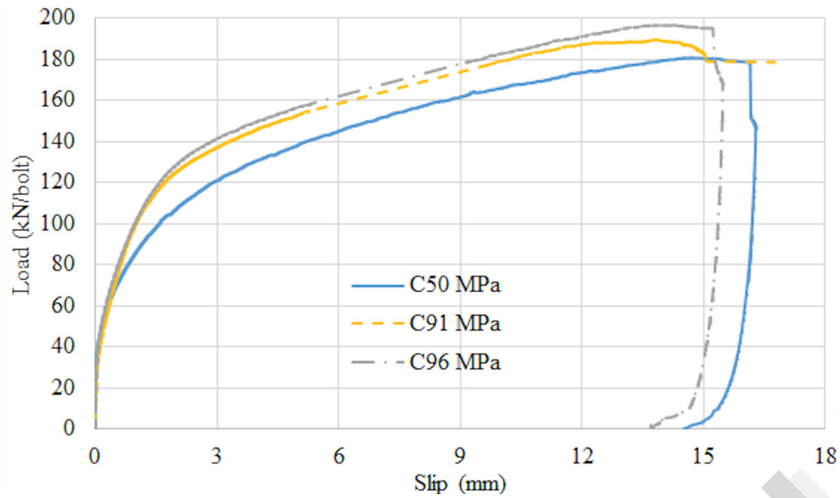

F24 : 1 **Fig. 24.** Effect of plug concrete strength on load-slip behavior (Tests 10, 11, and 12)

F25 : 1 **Fig. 25.** Effect of plug concrete strength on slab spalling

Effect of Plug Concrete Strength (Tests 9–12)

Push-out Tests 10–12 (Table 2) investigated the effect of plug concrete strength (i.e., 50, 91, and 96 MPa) on the LNSC behavior. Test 9 used plugs of 80-MPa concrete strength but failed due to accidental loss of bolt pretension; therefore, its results are not presented. The results of Tests 10–12 are presented in Table 9 and in Figs. 23–27.

Table 9 shows that changing the plug concrete compressive strength from C96 to C50 results in modest changes in the shear resistance (9% decrease) and slip capacity (5% increase) of the LNSC. These results further confirm that, unlike conventional studs, which have several modes of failure (BSI 1994), the LNSC has only one failure mode, i.e., shear failure of bolts just above the locking nuts.

Table 10 and Fig. 23 provide a comparison among the predictions for the shear resistance of the LNSC from Eq. (4) and the corresponding experimental values. It is shown that Eq. (4) provides good estimations with a maximum absolute error less than 8%. Eq. (4) predicts the shear resistance of the LNSC, which was obtained on the basis of standard push-out tests and specimen dimensions according to EC4 (BSI 2005b), for plug concrete strengths between 50 and 100 MPa, bolts with a steel strength of 889 MPa and diameter from 12 to 16 mm, grout compressive strength from 25 to 45 MPa, a full proof load (88–106 kN) between Nuts 1 and 2 (Fig. 4), and an initial internal bolt force equal to 25 kN.

Fig. 24 shows the effect of plug concrete strength on the shear load-slip displacement behavior. The plug concrete strength has no effect for loads up to 32% of the shear resistance, which is similar to welded studs (Oehlers and Coughlan 1986). An increase of the plug concrete strength from C50 to C96 increases the stiffness from 78 to 106 kN/mm at a shear load equal to 50% of the shear resistance. Fig. 25 shows the bottom face of the slabs after failure of the specimens of push-out Tests 10 and 11. Negligible differences can be noticed between the C50 and C96 plug concrete strength specimens. Moreover, Fig. 25 shows that spalling extends only within a 20-mm circular pattern inside the slabs.

Fig. 26 shows that as the plug concrete strength increases, less slab uplift displacement occurs. A 92% increase in plug concrete strength results in 33% reduction in uplift displacement at the onset of failure. Fig. 26 also highlights that slab separation starts for loads higher than 50% of the shear resistance and has a maximum value that is less than 0.5 mm at the onset of failure. These results further confirm that the LNSC has superior stiffness and strength against slab uplift.

Fig. 27 shows the deflected shape of bolts after failure of the specimens of push-out Tests 10–12. All bolts have similar deflected shapes, which is an observation that further indicates that plug concrete strength has little effect on the LNSC behavior.

Summary and Conclusions

A novel demountable LNSC for precast steel-concrete composite bridges has been presented. The LNSC uses high-strength steel bolts, which are fastened to the top flange of the steel beam using a locking nut configuration that prevents bolts from slipping inside their holes. Moreover, the locking nut configuration resembles in geometry the collar of welded shear studs and prevents local failure within the threaded part of the bolts to achieve higher shear resistance and ductility. The bolts are surrounded by conical precast high-strength concrete plugs, which have dimensions to easily fit within the precast slab pockets. Grout is used to fill all the gaps between the bolts, the precast plugs, and the precast slab pockets, whereas tightening of a nut at the top of the LNSC secures the plugs in place before grout hardening. Six preliminary push-out tests were conducted to fully illustrate why the novel structural details of the LNSC result in superior shear load-slip displacement behavior. Six additional push-out tests served to assess the repeatability in the LNSC behavior as well as to quantify the effects of the bolt diameter and the concrete plug strength. A simple design equation to predict the shear resistance of the LNSC was proposed. Based on the results presented in the paper, the following conclusions are drawn:

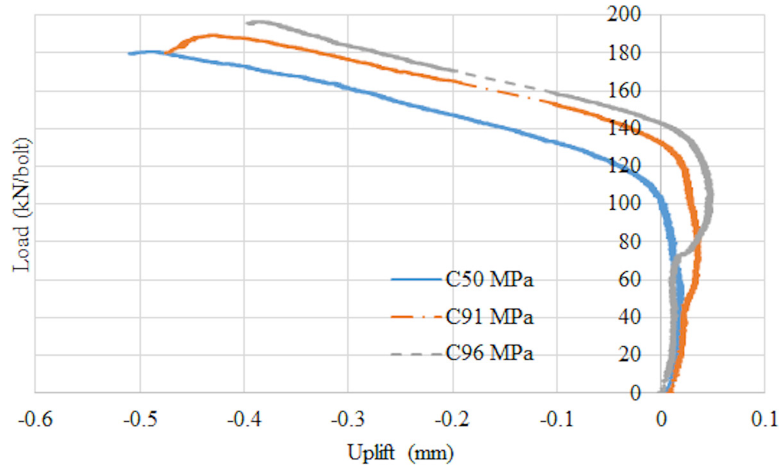

F26 : 1 **Fig. 26.** Effect of plug concrete strength on slab uplift displacement (Tests 10, 11, and 12)

F27 : 1 **Fig. 27.** Deflected shapes of M16 bolts for different plug concrete strengths

Table 10. Comparison among the Predictions of Eq. (4) and the Push-Out Tests Results

Test number	Bolt diameter (mm)	Plug strength (MPa)	Ultimate load (kN)	Eq. (4) (kN)	Error %
7	12	91	99.3	107.6	8.0
8	14	95	155.2	149.2	−4.0
10	16	50	180.7	190.7	6.0
11	16	96	196.7	195.5	−1.0
12	16	91	189.5	196.8	4.0

1. The LNSC allows rapid bridge disassembly and easy replacement of any deteriorating structural component (i.e., precast deck panel, shear connector, steel beam). Therefore, the use of the LNSC in practice can result in significant reduction of the lifecycle direct and indirect socioeconomic costs related to maintenance, repair, or replacement of precast steel-concrete composite bridges.
2. The LNSC promotes accelerated bridge construction by taking full advantage of prefabrication. In particular, fabrication of all structural components is performed in the shop and only the final assembly between the precast slab and the steel beam is performed on-site. Moreover, the latter does not involve working underneath the bridge deck.
3. The LNSC has very high shear resistance and stiffness, leading to reduction of the required number of shear connectors and slab pockets compared with welded studs or previously proposed bolted shear connectors. The characteristic shear resistance and stiffness of the LNSC for an M16 bolt were found equal to 170.5 kN and 100 kN/mm, respectively.
4. The LNSC has very large slip capacity, i.e., up to 14.0 mm.
5. The LNSC has superior stiffness and strength against slab uplift compared with welded studs, e.g., the uplift displacement is less than 4% of the corresponding slip displacement at shear load equal to 80% of the shear resistance.
6. The shear load-slip displacement behavior of the LNSC shows repeatability and negligible scatter. Among three identical push-out tests, the maximum deviations of any individual test from the average were only 2 and 6% for the shear resistance and slip capacity, respectively.
7. Increasing the plug concrete strength from C50 to C96 was found to have negligible effect on shear resistance (9% increase) and slip capacity (5% decrease).
8. The proposed design equation [Eq. (4) in the paper] was checked against test results of specimens with different bolt diameters and plug concrete strengths and was found to

predict the shear resistance of the LNSC with maximum absolute error less than 8%.

9. The shear resistance of the LNSC could be approximately considered equal to 1.1 times the bolt tensile resistance for preliminary design purposes.
10. More parametric push-out tests and fatigue tests should be conducted to confirm and extend the knowledge on the LNSC behavior. Moreover, full-scale precast steel-concrete composite beam tests are needed to assess the behavior of the LNSC within boundary conditions similar to those encountered in practice.

Acknowledgments

This work was financially supported by the Iraqi Ministry of Higher Education and Scientific Research (Ph.D. scholarship to the first author) and from the University of Warwick through its Strategic EPSRC Impact Fund (awarded to the second author). Hanson Cement & Packed Products Ltd. and Grace Construction Products Ltd. donated raw materials for the fabrication of the test specimens. Emeritus Professor Roger P. Johnson of the University of Warwick kindly reviewed interim technical reports and offered comments and advices of significant value. Dr. Melody Stokes of Warwick Ventures Ltd. facilitated the process of receiving constructive feedback from international structural engineering consulting firms. Technical staff of the University of Warwick provided valuable help with the experimental setup and program. The authors gratefully acknowledge the previously mentioned support. Any opinions, findings, and conclusions expressed in this paper are those of the authors and do not necessarily reflect the views of the previously mentioned sponsors and supporters.

References

ASCE. (2014). "Infrastructure report card: A big win for water resources." ⟨http://www.infrastructurereportcard.org/a/#p/bridges/conditions-and-capacity⟩ (Oct. 23, 2016).

Ataei, A., Bradford, M. A., and Liu, X. (2016). "Experimental study of composite beams having a precast geopolymer concrete slab and deconstructable bolted shear connectors." *Eng. Struct.*, 7, 1–13.

Badie, S. S., and Tadros, M. K. (2008). *Full-depth precast concrete bridge deck panel systems*, Transportation Research Board, Washington, DC.

Ban, H., Uy, B., Pathirana, S. W., Henderson, I., Mirza, O., and Zhu, X. (2015). "Time-dependent behaviour of composite beams with blind bolts under sustained loads." *J. Constr. Steel Res.*, 112(Sep), 196–207.

Biswas, M. (1986). "On modular full depth bridge deck rehabilitation." *J. Transp. Eng.*, 10.1061/(ASCE)0733-947X(1986)112:1(105), 105–120.

BSI (British Standards Institution). (1970). "Specification for wheels for agricultural machinery, implements and trailers. Part 3: Nuts." *BS 3486-3*, London.

BSI (British Standards Institution). (1976). "Specifications for building sands from natural sources." *BS 1199*, London.

BSI (British Standards Institution). (1979). "Steel, concrete and composite bridges. Part 5: Code of practice for design of composite bridges." *BS 5400-5*, London.

BSI (British Standards Institution). (1994). "Draft for development: Eurocode 4: Design of composite steel and concrete structures. Part 1-1: General rules and rules for buildings." *BS EN 1994-1-1*, London.

BSI (British Standards Institution). (2004). "Eurocode 4: Design of composite steel and concrete structures. Part 1-1: General rules and rules for buildings." *BS EN 1994-1-1*, London.

BSI (British Standards Institution). (2005a). "Eurocode 3: Design of steel structures. Part 1-1: General rules and rules for buildings." *BS EN 1994-1-1*, London.

BSI (British Standards Institution). (2005b). "Eurocode 4: Design of composite steel and concrete structures. Part 1-2: General rules and rules for bridges." *BS EN 1994-2*, London.

BSI (British Standards Institution). (2005c). "High-strength structural bolting assemblies for preloading. Part 3: System HR, hexagon bolt and nut assemblies." *BS EN 14399-3*, London.

BSI (British Standards Institution). (2005d). "High-strength structural bolting assemblies for preloading. Plain chamfered washers." *BS EN 14399-6*, London.

BSI (British Standards Institution). (2009a). "High-strength structural bolting assemblies for preloading. Part 9: System HR or HV–direct tension indicators for bolt and nut assemblies." *BS EN 14399-9*, London.

BSI (British Standards Institution). (2009b). "Metallic materials–tensile testing. Part 1: Method of test at ambient temperature." *BS EN ISO 6892-1*, London.

Chen, Y.-T., Zhao, Y., West, J. S., and Walbridge, S. (2014). "Behaviour of steel–precast composite girders with through-bolt shear connectors under static loading." *J. Constr. Steel Res.*, 103(Dec), 168–178.

Dai, X., Lam, D., and Saveri, E. (2015). "Effect of concrete strength and stud collar size to shear capacity of demountable shear connectors." *J. Struct. Eng.*, 10.1061/(ASCE)ST.1943-541X.0001267, 04015025.

Dallam, L. N. (1968). "High strength bolt shear connectors–pushout tests." *ACI J.*, 65(9), 767–769.

Dallam, L. N., and Harpster, J. L. (1968). "Composite beam tests with high-strength bolt shear connectors." *Rep. 68-3*, Dept. of Civil Engineering, Univ. of Missouri, Columbia, MO.

Deng, Y., Phares, B., Dang, H., and Dahlberg, J. (2016). "Impact of concrete deck removal on horizontal shear capacity of shear connections." *J. Bridge Eng.*, 10.1061/(ASCE)BE.1943-5592.0000832, 04015059.

Hallmark, R. (2012). "Prefabricated composite bridges–a study of dry joints." Licentiate thesis, Dept. of Civil, Mining and Natural Resources Engineering, Lulea Univ. of Technology, Lulea, Sweden.

Henderson, I. E. J., Zhu, X. Q., Uy, B., and Mirza, O. (2015a). "Dynamic behaviour of steel-concrete composite beams with different types of shear connectors. Part I: Experimental study." *Eng. Struct.*, 103, 298–307.

Henderson, I. E. J., Zhu, X. Q., Uy, B., and Mirza, O. (2015b). "Dynamic behaviour of steel-concrete composite beams with different types of shear connectors. Part II: Modelling and comparison." *Eng. Struct.*, 103, 308–317.

Johnson, R. P. (1967). *Structural concrete*, McGraw-Hill, Berkshire, U.K., 32.

Johnson, R. P. (1981). "Loss of interaction in short-span composite beams and plates." *J. Constr. Steel Res.*, 1(2), 11.

Johnson, R. P. (2004). *Composite structures of steel and concrete: Vol. 1: Beams, slabs, columns, and frames for buildings*, 3rd Ed., Blackwell Scientific, Oxford, U.K., 32.

Johnson, R. P. (2012). *Designers' guide to Eurocode 4: Design of composite steel and concrete structures*, 2nd Ed., Thomas Telford, London, 213.

Johnson, R. P., and Buckby, R. J. (1986). "Composite structures of steel and concrete: Vol. 2: Bridges." *Collins professional and technical books*, 2nd Ed., London, 63.

Johnson, R. P., and May, I. M. (1975). "Partial-interaction design of composite beams." *Struct. Engineer*, 53(8), 305–311.

Kwon, G., Engelhardt, M., and Klingner, R. (2011). "Experimental behavior of bridge beams retrofitted with postinstalled shear connectors." *J. Bridge Eng.*, 10.1061/(ASCE)BE.1943-5592.0000184, 536–545.

Kwon, G., Engelhardt, M. D., and Klinger, R. E. (2010). "Behavior of post-installed shear connectors under static and fatigue loading." *J. Constr. Steel Res.*, 66(4), 532–541.

Lin, Z., Liu, Y., and He, J. (2014). "Behavior of stud connectors under combined shear and tension loads." *Eng. Struct.*, 81(Dec), 362–376.

Liu, X., Bradford, M., and Lee, M. (2014). "Behavior of high-strength friction-grip bolted shear connectors in sustainable composite beams." *J. Struct. Eng.*, 10.1061/(ASCE)ST.1943-541X.0001090, 04014149.

Marshall, W. T., Nelson, H. M., and Banerjee, H. K. (1971). "An experimental study of the use of high strength friction grip bolts as shear connectors in composite beams." *Struct. Engineer*, 49(4), 175.

Moynihan, M. C., and Allwood, J. M. (2014). "Viability and performance of demountable composite connectors." *J. Constr. Steel Res.*, 99(Aug), 47–56.

Oehlers, D. J. (1980). “Stud shear connectors for composite beams.” Ph.D. thesis, School of Engineering, Univ. of Warwick, Coventry, U.K.

Oehlers, D. J., and Bradford, M. A. (1995). *Composite steel and concrete structural members: Fundamental behavior*, Elsevier Science Ltd, Oxford, U.K.

Oehlers, D. J., and Bradford, M. A. (1999). *Elementary behavior of composite steel & concrete structural members*, Butterworth-Heinemann, Oxford, U.K., 84–94.

Oehlers, D. J., and Coughlan, C. G. (1986). “The shear stiffness of stud shear connections in composite beams.” *J. Constr. Steel Res.*, 6(4), 273–284.

PANTURA. (2011). “Needs for maintenance and refurbishment of bridges in urban environments.” ⟨http://www.pantura-project.eu/Downloads/D5.3.pdf⟩ (Oct. 23, 2016).

Pathirana, S. W., Uy, B., Mirza, O., and Zhu, X. (2015). “Strengthening of existing composite steel-concrete beams utilising bolted shear connectors and welded studs.” *J. Constr. Steel Res.*, 114(Nov), 417–430.

Pathirana, S. W., Uy, B., Mirza, O., and Zhu, X. (2016). “Flexural behaviour of composite steel-concrete utilising blind bolt shear connectors.” *Eng. Struct.*, 114(May), 181–194.

Pavlović, M., Marković, Z., Veljković, M., and Buđevac, D. (2013). “Bolted shear connectors vs. headed studs behaviour in push-out tests.” *J. Constr. Steel Res.*, 88(Sep), 134–149.

Pavlović, M. S. (2013). “Resistance of bolted shear connectors in prefabricated steel-concrete composite decks.” Ph.D. thesis, Univ. of Belgrade, Faculty of Civil Engineering, Belgrade, Serbia.

Shim, C.-S., Lee, P.-G., and Chang, S.-P. (2001). “Design of shear connection in composite steel and concrete bridges with precast decks.” *J. Constr. Steel Res.*, 57(3), 203–219.

Spremić, M., Marković, Z., Veljković, M., and Budjevac, D. (2013). “Push–out experiments of headed shear studs in group arrangements.” *Adv. Steel Constr.*, 9(2), 170–191.

Tadros, M. K., and Baishya, M. C. (1998). “Rapid replacement of bridge decks.” *NCHRP Rep. 407*, Transportation Research Board, Washington, DC.

Vayas, I., and Iliopoulos, A. (2014). *Design of steel-concrete composite bridges to Eurocodes*, CRC Press/Taylor & Francis Group, Boca Raton, FL, 490.

Wallaert, J. J., and Fisher, J. W., (1964). “Shear strength of high-strength bolts.” Paper 1822, Fritz Laboratory Reports, Lehigh Univ., Bethlehem, PA.

Xue, W., Ding, M., Wang, H., and Luo, Z. (2008). “Static behavior and theoretical model of stud shear connectors.” *J. Bridge Eng.*, 10.1061/(ASCE)1084-0702(2008)13:6(623), 623–626.

Yam, L. C. P. (1981). *Design of composite steel-concrete structures*, Surrey University Press, London, 75.

AUTHOR QUERY FORM

AQ1: ASCE Open Access: Authors may choose to publish their papers through ASCE Open Access, making the paper freely available to all readers via the ASCE Library website. ASCE Open Access papers will be published under the Creative Commons-Attribution Only (CC-BY) License. The fee for this service is $1750, and must be paid prior to publication. If you indicate Yes, you will receive a follow-up message with payment instructions. If you indicate No, your paper will be published in the typical subscribed-access section of the Journal.

AQ2: Please provide the ASCE Membership Grades for the authors who are members.

AQ3: First affiliation: Please add a city for the Univ. of Warwick affiliation.

AQ4: Please provide details of the citation [Suwaed et al. (2016)] in the reference list.

AQ5: Please add a manufacturer's address (city and state) for Grace Construction Products.

AQ6: ASCE (2014) reference: Please confirm the changes made in the URL title.

AQ7: Pantura (2011): please provide a URL that takes the reader directly to the document being cited.